OPERATION AND DEVELOPMENT OF THE FLNR ACCELERATOR COMPLEX (DRIBs-III)

Employing the FLNR cyclotrons DC-280, U-400, U-400M, a wide variety of scientific and applied investigations in heavy-ion physics were conducted. The operating hours of the cyclotrons are shown in Fig. 1.

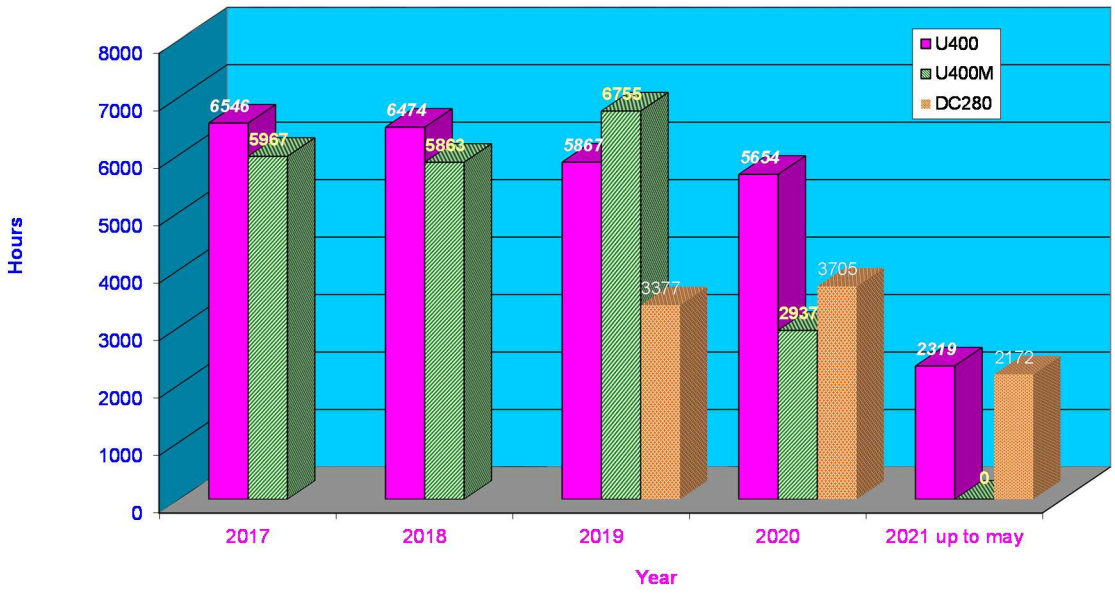

Fig.1. Operating hours of U400, U400M, and DC280 cyclotrons in 2017 – 2021

The DC280 cyclotron for the Factory of superheavy elements

Since 1998 priority experiments on synthesis of new superheavy elements (SHE) with atomic numbers of 114-118 in reactions of ^{48}Ca ions with actinide targets (^{242,244}Pu, ^{243}Am, ^{249}Cm, ^{249}Bk, ^{249}Cf) have been carried out at the FLNR JINR on the U-400 accelerating complex. Over 50 new isotopes of elements 104 to 118 with maximum neutron excess were for the first time produced and their decay properties were determined in these investigations. The International Unions of pure and applied physics (IUPAP) and chemistry (IUPAC) recognized the priority of Dubna in the discovery of elements 114-118. The seventh period of the Periodic Table has been completed. The discovery of the new domain (island) of stability and the very fact of existence of SHE have posed a number of new questions associated with fundamental properties of nuclear matter. Can even heavier nuclei exist? Is the "Island of Stability of SHE the last one on the Chart of the Nuclides? Can the superheavy nuclei be formed in the process of nucleosynthesis like those stable and long-lived nuclei in the groups of Pt, Pb, and U-Th found in Nature? What is the limit of Mendeleev's Table? How much are the chemical properties of SHE similar to those of their lighter homologues? Direct synthesis of elements

with Z >118 in fusion reactions means using projectiles heavier than Ca, since the capability of high-flux reactors to produce target material is limited to Cf isotopes. It is expected that production cross sections of nuclei with Z=120 in the reaction $^{54}Cr+^{248}Cm$ and nuclei with Z = 119 via $^{50}Ti+^{249}Bk$ will be ten to twenty times lower than those of production of isotopes of elements 114 and 115 in experiments with ^{48}Ca. For more detailed studying nuclear - physical and chemical properties of SHE it was necessary significantly increasing efficiency of experiments [1]. For the solution of this task the first in the world Factory of superheavy elements (SHE Factory) was created at the FLNR JINR in 2019.

Development of the SHE Factory was associated with extending the FLNR experimental basis in several directions. These directions are:

- creation of the new DC280 accelerator of stable and long-living isotopes with masses range A = 4÷238 with intensity up to 10 pμA for A≤50 and energy up to 8 MeV/nucleon;
- construction of a new experimental building and infrastructure for placing the accelerator with five channels for transportation of beams to 3 experimental halls (total area up to 1000 m^2), equipped with systems of shielding and control matching the class two of operations with radioactive materials;
- development of new separators, development of new detection modules for the study of nuclear, atomic, and chemical properties of new elements;
- production of new target materials and development of techniques of making targets with high thermal and radiation stability.

The SHE Factory was constructed in the new stand-alone experimental building (Fig.2).

Fig. 2. Building of SHE Factory

The basic facility of the SHE Factory—DC280 cyclotron—was finally assembled, adjusted, tested (2017-2018) [2] and officially commissioned on 25 March 2019 (fig.3) [3].

Fig. 3. The opening ceremony of the DC-280 cyclotron

The main parameters of the cyclotron specified in Table 1. Configuration of the DC280 cyclotron shown in Fig. 4. The DC280 equipped with the high voltage injection system which arranged above the main magnet. The system consists of the high voltage (HV) platform with the DECRIS-PM ECR ion source, the maximal voltage at the platform is 70 kV. The DECRIS-PM is the source with permanent magnet structure created at the FLNR [4]. The source extraction voltage is up to 20 kV. The cyclotron has a compact type magnet. The magnetic structure consists of four pairs of focusing sectors. The wide range of the magnetic field levels 0.64÷1.32 T allows to make smooth variation of the beam energy in a range 4÷8 MeV/n. For optimization of the magnetic field the 11 radial correcting coils are utilized. Accelerating system of the DC280 consists of two main 45° dees and two flat-top 20° dees combined with RF- resonators. The ion beam extraction system of the DC280 equipped with the electrostatic deflector and the passive focusing magnetic channel. Extracted ion beams can be transported along five beam transport lines.

Table 1: Main Parameters of DC280

Parameter	**Value**
Injecting beam potential	Up to 80 kV
Pole diameter	4 m
A/Z range of ions	4÷7.5
Magnetic field	0.6÷1.3 T

K factor	280
Magnet weight	1100 t
Magnet power	300 kW max
Dee voltage	2x130 kV
Flat-top dee voltage	2x13 kV
Deflector strength	90 kV/cm max

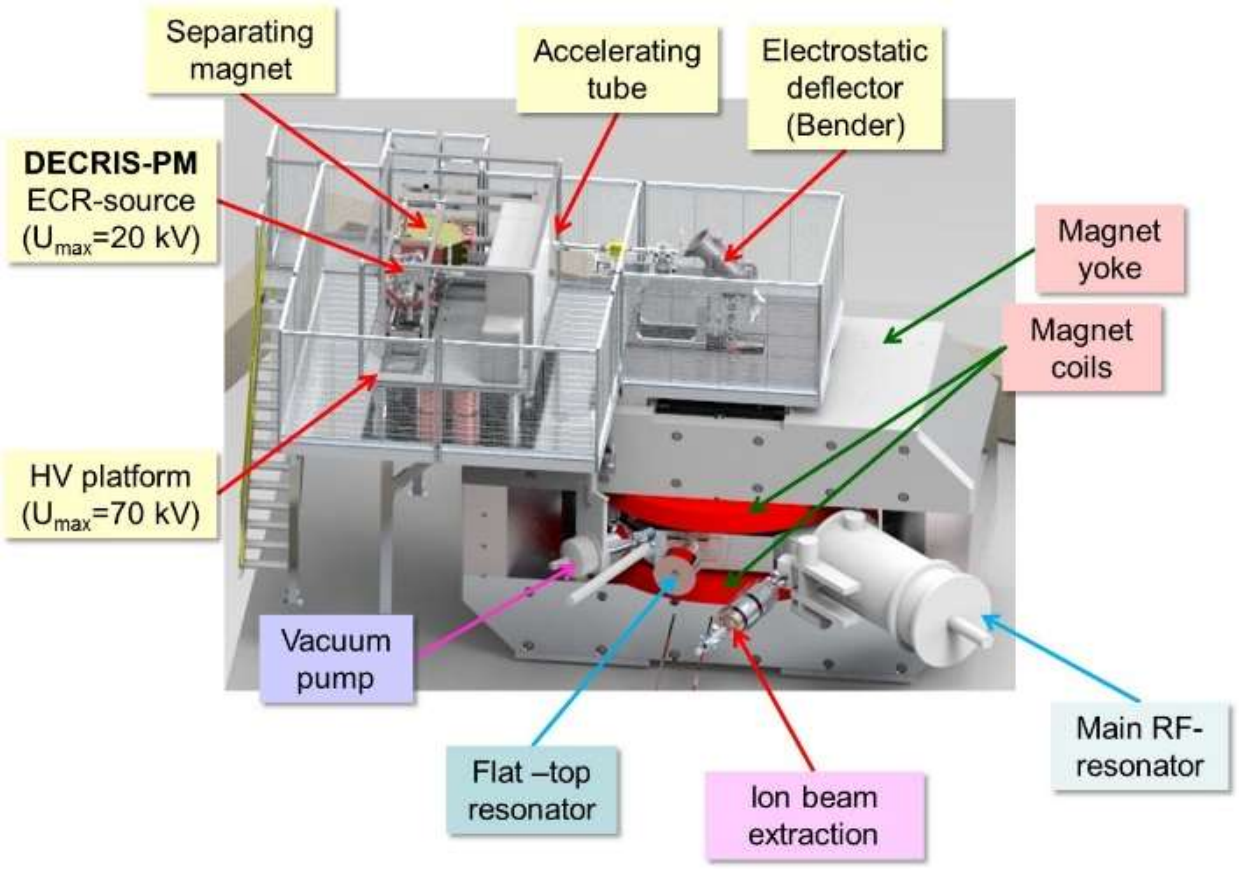

Fig.4. DC280 configuration.

Working diagram of the DC280 (Fig. 5) shows the dependence of ion energies on A/Z (atomic mass to charge ratio). The points correspond to accelerated ions.

For today, the maximal extracted intensities are: 10 pμA for $^{12}C^{+2}$ (beam power is P_{beam}=0.71 kW), 10.4 pμA for $^{40}Ar^{+7}$ (P_{beam}=2.04 kW), 7.1 pμA for $^{48}Ca^{+10}$ (P_{beam}= 1.64 kW), 1 pμA for $^{48}Ti^{+10}$ (P_{beam}=0,23 kW), 2.4 pμA for $^{52}Cr^{+10}$ (P_{beam}=0.65 kW) and 1.4 pμA for $^{84}Kr^{+14}$ (P_{beam}=0.69 kW) (Tab. 2). The DC-280 works for physical experiments on the synthesis of element 114 (flerovium) in the ^{242}Pu + ^{48}Ca reaction and element 115 (moscovium) in the ^{243}Am + ^{48}Ca reaction. The ways of the further increase of beam intensities, first of all of titanium and chromium, are being studied.

Table 2. Experimental ion beam parameters of DC280

Ion	E_{ion} [Mev/nucl.]	I_{INJ} [pμA]	I_{EXTR} [pμA]
$^{12}C^{+2}$	5.9	29,8	10
$^{40}Ar^{+7}$	4.9	28.7	10.4
$^{48}Ca^{+10}$	4.8	24	7.1
$^{48}Ti^{+10}$	4.8	2.2	1
$^{52}Cr^{+10}$	5.2	7	2.4
$^{84}Kr^{+14}$	5.9	2.9	1.4

I_{INJ}- ion current in the injection channel, I_{EXTR}- ion current extracted from the DC280.

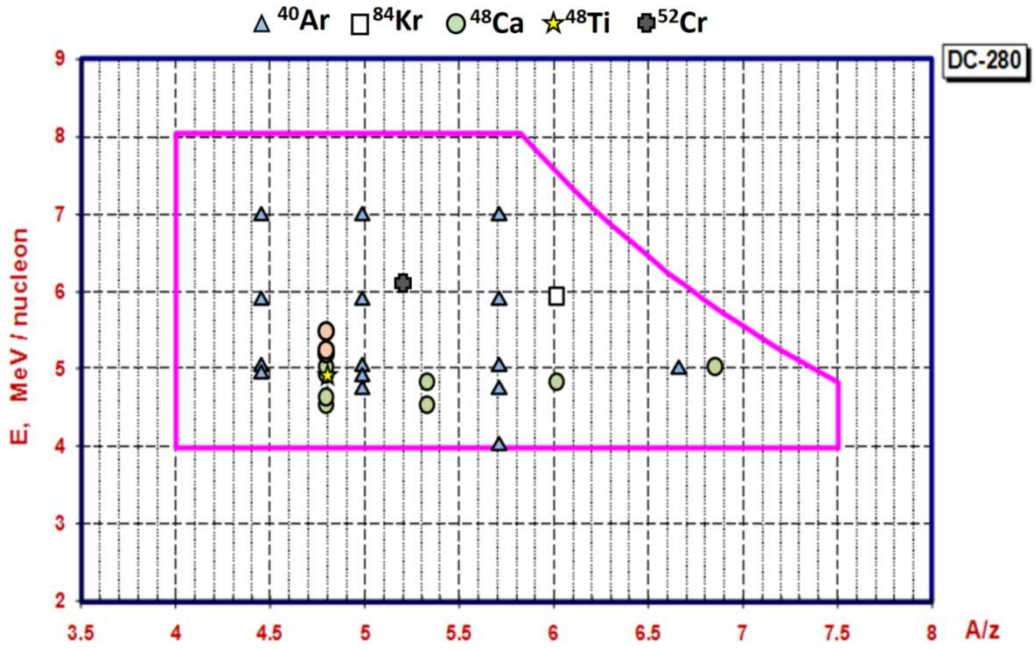

Fig. 5. Working diagram of the DC280 cyclotron with points corresponding to accelerated ions

References

[1] Sergey Dmitriev, Mikhail Itkis and Yuri Oganessian, Status and perspectives of the Dubna superheavy element factory, in Proceedings of the Nobel Symposium NS 160, EPJ Web of Conferences 131 08001, 2016, p. 1-6.

[2] G. G. Gulbekian, S. N. Dmitriev, M. G. Itkis, Yu. Ts. Oganessyan, B. N. Gikal, I. V. Kalagin,V. A. Semin, S. L. Bogomolov, V. A. Buzmakov, I. A. Ivanenko, N. Yu. Kazarinov, N. F. Osipov,S. V. Pashenko, V. A. Sokolov, N. N. Pchelkin, S. V. Prokhorov, M.V. Khabarov, K.B. Gikal, Start-Up of the DC-280 Cyclotron, the Basic Facility of the Factory of Superheavy Elements of the Laboratory of Nuclear Reactions at the Joint Institute for Nuclear Research, ISSN 1547-4771, Physics of Particles and Nuclei Letters, 2019, Vol. 16, No. 6, pp. 866–875.

[3] S.N. Dmitriev, Yu.Ts. Oganessian, G.G. Gulbekyan, I.V. Kalagin, B.N. Gikal, S.L. Bogomolov, I.A. Ivanenko, N.Yu. Kazarinov, G.N. Ivanov, N.F. Osipov, S.V. Pashchenko, M.V. Khabarov, V.A. Semin, A.V. Yeremin, V.K. Utyonkov, SHE Factory: cyclotron facility for super heavy elements research // Proceedings of CYC19 Int. Conf., South Africa, Cape Town, 2019, P. 305-309.

[4] S.L. Bogomolov, A.E. Bondarchenko, A.A. Efremov, K.I. Kuzmenkov, A.N. Lebedev, V.E. Mironov, V.N. Loginov, N.Yu. Yazvitsky, N.N. Konev, Production of High-Intensity Ion Beams from the DECRIS-PM-14 ECR Ion Source, Physics of Particles and Nuclei Letters, Vol. 15, No. 7, 2018, p. 878–881.

U-400 cyclotron

The program for experimental investigations at the FLNR U-400 accelerator complex was implemented according to the plan. The operation time of the U400 cyclotron in 2017- 2021 is shown in Fig.1. The operation time of the U400 cyclotron was used mainly for implementation of the research program with beams of ^{48}Ca (the DGFRS and the SHELS setups) and ^{50}Ti (the SHELS setup). Contract obligations of FLNR JINR (ROSCOSMOS) were completely fulfilled on time.

U400M cyclotron

The U400M cyclotron had operated till the start of its modernization in July 2020 (Fig.1). The U400M cyclotron provides the beams of ^{11}B,^{15}N,^{32}S delivered to the ACCULINNA-1,2 separators, ^{18}O,^{22}Ne to the COMBAS setup and ^{40}Ar,^{48}Ca to the MASHA mass-spectrometer. The upgrade of the cyclotron will last till mid of 2022. The cyclotron components, parts of beam lines, outdated vacuum and water cooling system equipment were dismantled. Today, the process of dismantling the old winding (Fig. 6) and preparing for the installation of the new one is underway, and the work is being carried out under the contract with the GKMP, Bryansk. A new control system is being developed; new components of the cyclotron are designed and manufactured. The modernization aims at enhancing the reliability and stability of the accelerator (replacement of the main magnet coils, accelerator vacuum system components, control system and radiation control system) as well as increasing the intensity and energy of heavy-ion beams.

Fig. 6. Dismantling of the U400M main winding

Development of the DC-140 cyclotron complex

Development of the cyclotron complex DC-140 [1] intended for applied studies is underway in the Flerov Laboratory since 2020. The main goals of the project include studies within solid state physics, surface modifications of materials, production of track membranes and testing of electronic components for single radiation effects (SEE testing).

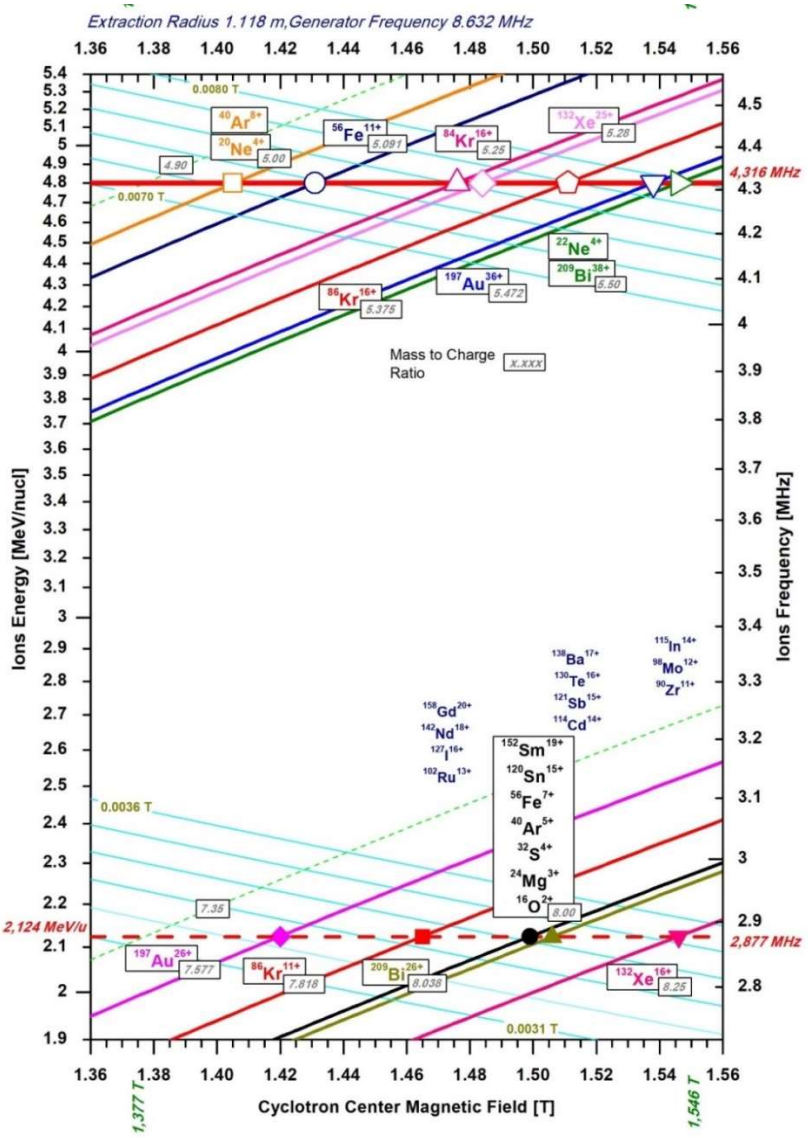

Fig. 7. Working diagram of the DC-140 cyclotron

The complex is based on the operation of the dedicated compact DC-140 cyclotron. We are planning that upon the launch, the cyclotron DC-140 will replace the cyclotron IC-100 in applied studies carried out in the FLNR. Construction of the DC-140 cyclotron complex is planned to be completed by the end 2023. Conceptual design of the cyclotron complex and the study of its feasibility have been performed in 2020. Design work continues in 2021.

Cyclotron DC-140 is intended for the acceleration of ion beams from O to Bi with energies 4.8 and 2.1 MeV/n (Fig. 7). Beams of lower energy are assumed to be used to produce track membranes based on polymer films up to 30 μm thick. Ion beams with the energy 4.8 MeV/n will provide a depth of ion penetration in Si up to 55 μm and LET in Si up to 100 MeV*cm^2/mg for effective SEE testing. The working diagram of cyclotron DC-140 is shown in Fig.7.

Three dedicated beam-channels are planned to be installed at the DC-140 cyclotron, including upgraded operating channel for irradiation of polymeric materials (Fig. 8).

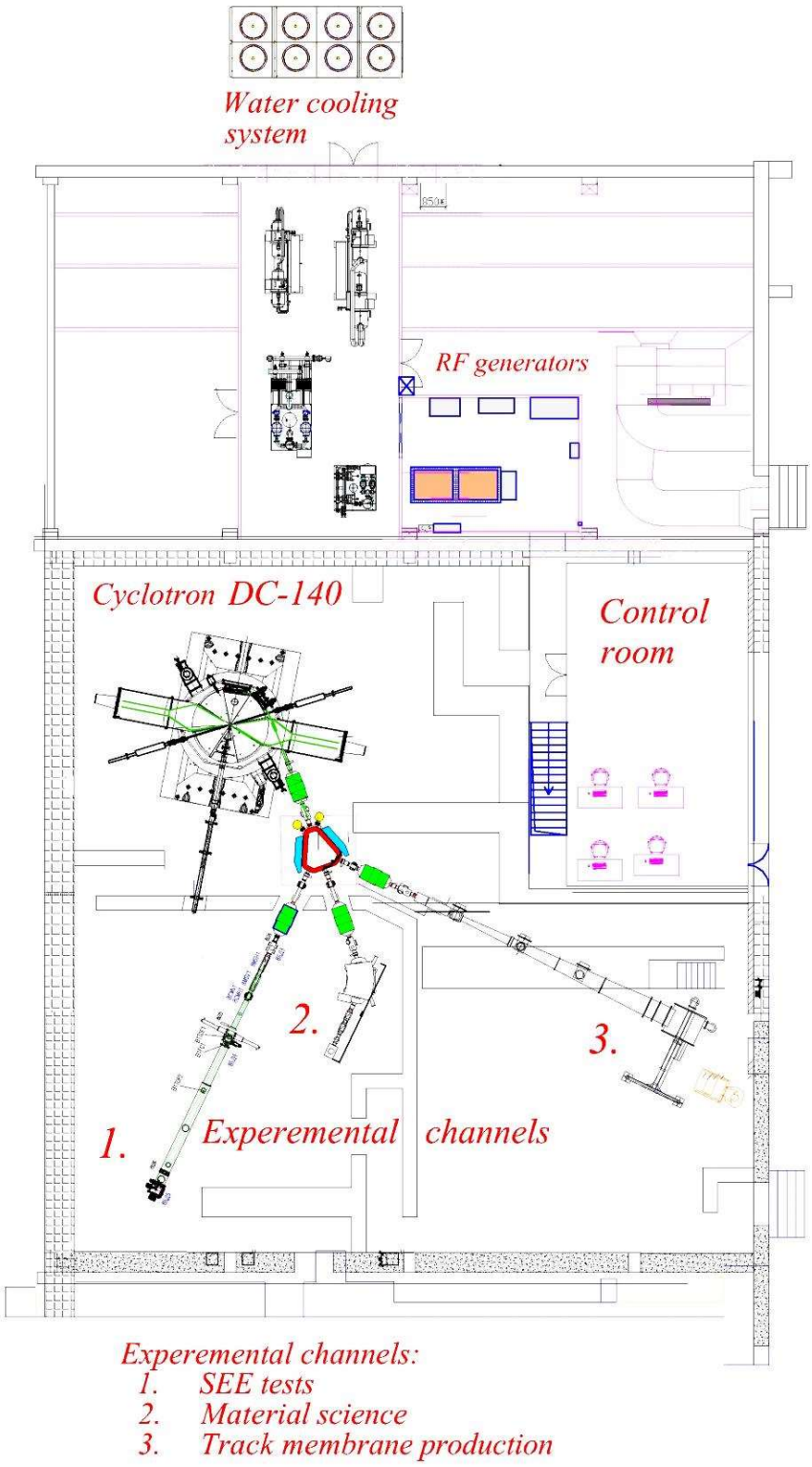

Fig. 8. Layout of the DC-140 cyclotron complex

References

[1] S. Mitrofanov, P. Apel, V. Bashevoy, V. Bekhterev, S. Bogomolov, O. Borisov, J. Franko, B. Gikal, G. Gulbekyan, I. Ivanenko, I. Kalagin, N. Kazarinov, V. Mironov, V. Semin, V. Skuratov, A. Tikhomirov, FLNR JINR accelerator complex for applied physics researches: state-of-art and future // Proceedings of CYC19 Int. Conf., South Africa, Cape Town, 2019, pp. 358-360

The new assembly hall

The construction of the new assembly hall (fig. 9) is finished in May 2021, which is essential, in particular, for the implementation of the FLNR plans to develop and upgrade the fleet of cyclotrons.

Fig. 9. The new assembly hall

Reconstruction of the U400R cyclotron

Within preparation for the reconstruction of the U400R cyclotron, the project of the New Experimental Hall of U-400R was prepared (see fig. 10). In 2021 the project received a positive conclusion from the Glavgosexpertiza (Main Department of State Expertise) of Russia. At present, the working project for the new Experimental Hall is being created. The planned construction period is 2.5 years (2022-2024).

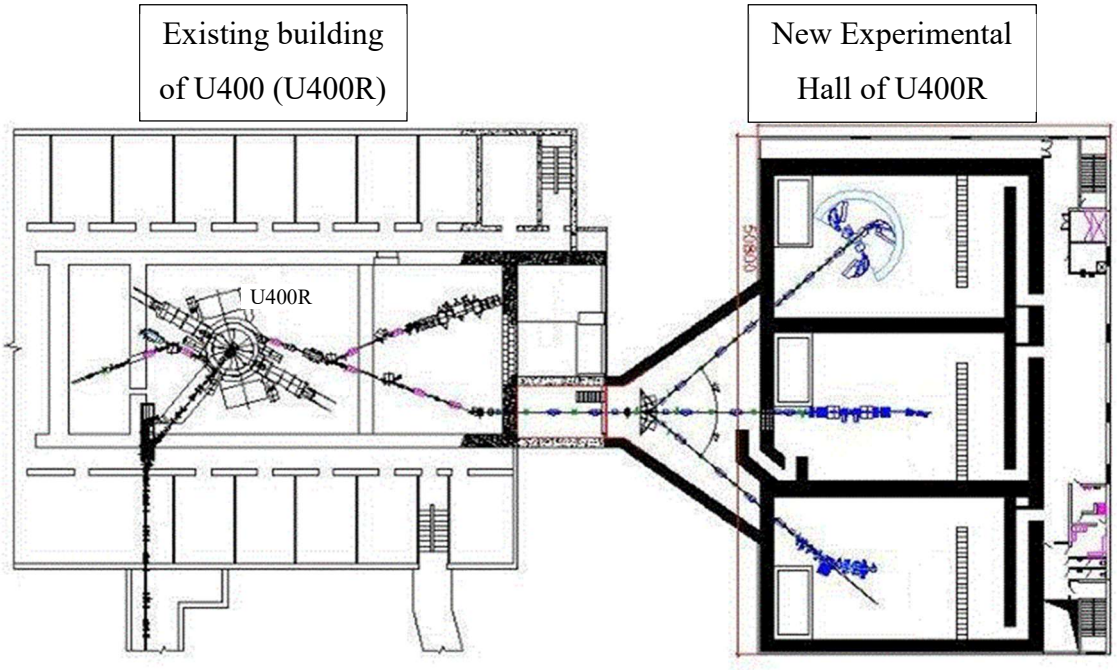

Fig. 10. The new experimental building of U400R (on the right).

DEVELOPMENT OF EXPERIMENTAL PHYSICAL SETUPS

Construction and commissioning of the new gas-filled separator DGFRS-2

The first experimental facility, aimed at continuing the study of the superheavy nuclei at the SHE Factory of FLNR, JINR, is a new gas-filled separator DGFRS-2. The separator was designed in FLNR and manufactured by SIGMAPHI (France). In 2018, the installation of the main components of the separator had been completed. The first quadrupole lens Q_1 focuses vertically on the nuclei knocked out of the target to increase the efficiency of their transport through the gap of the magnet D_1, where the products of the complete-fusion reactions (ERs) are separated from the bulk of the beam particles and the products of background reactions. The ERs are then focused on two quadrupole lenses Q_2 and Q_3. The magnet D_2 is installed for additional separation of ERs from background particles.

Other essential components of DGFRS-2 have been designed and manufactured: these are the system of differential pumping of gas that is to provide a gradient of pressure from 1 Torr in the separator to 10^{-7} Torr in the beam line and the target modules. At the end of 2018, the detection system module and the supports for the parts of the beamline have been delivered.

In 2019 the work on commissioning of all the units of the separator DGFRS-2 (Fig. 11) was completed. All the beam line elements are mounted ahead of the separator. Components have been developed and installed for control of the vacuum systems of the beam line and separator, for measuring the parameters of the ion beam, for supplying gas in the separator, for control of the magnetic elements, control and safety components of the vacuum systems.

The characteristics of dipole and quadrupole magnets, as well as distances, are summarized in Tables 3, 4, and 5, respectively.

Table 3. Characteristics of dipole magnets.

Magnet	D1	D2
Bending angle (deg)	31.5	10
Bending radius (m)	1.86	2.58
Pole gap [a)] (mm)	132	120
Maximum field (T)	1.80	1.81
Entrance angle (deg)	-8.4	0
Exit angle (deg)	-44.5	0
Dispersion (mm/%Bρ)	32.8	2.40

[a)] Gaps in reaction chambers are 120 mm for D1 and 108 mm for D2.

Table 4. Characteristics of quadrupole magnets.

Magnet	$Q1_v$	$Q2_h$	$Q3_v$
Maximum field gradient (T/m)	13.3	5.4	5.4
Bore radius (mm)	75	150	150
Pole length (mm)	420	520	520
Effective length (mm)	456	600	601

Table 5. Distances in [mm] [a].

Target – Q1	734
Q1 – D1	1170
D1 – Q2	1795
Q2 – Q3	1000
Q3 – D2	1457
D2 – Mylar	916
Mylar – DSSD array	335
Target – DSSD array	7407

[a] The distances correspond to the middles of the dipoles and quadrupoles.

The first test experiments were carried out in order to determine the optimum parameters of the DGFRS-2 using α particles and products of the reaction ^{nat}Yb(^{40}Ar,*xn*)$^{207\text{-}212}$Ra. Experiments were launched with the ^{48}Ca beam and targets of ^{nat}Yb, ^{174}Yb, ^{170}Er.

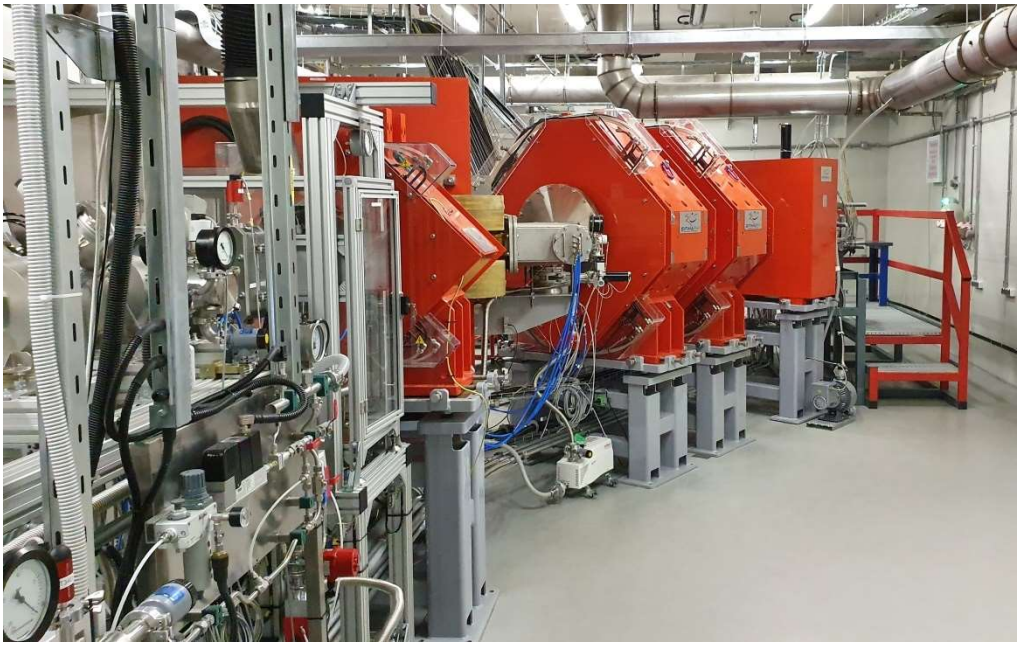

Fig. 11. The gas-filled separator DGFRS-2.

In 2020, test experiments were continued with an aim to determine the optimum parameters of the DGFRS-2 gas-filled separator for transporting the reaction products of ^{48}Ca with targets of ^{nat}Yb, ^{174}Yb, ^{170}Er, and ^{206}Pb. These tests are required for preparing experiments on synthesis and study of the superheavy nuclei (SHN). This series of experiments have shown that for a more efficient collection of nuclei, it is necessary to increase the detector size in the separator's focal plane. A new system of detectors with a size of 48 mm×220 mm was developed, assembled, and tested (Fig. 12). This makes it possible to increase the collection efficiency of reaction products by a factor of 1.5, which is of extreme importance for running long-term experiments on the synthesis of SHN. With these new detectors, we determined the optimum setting of DGFRS-2, the dispersion of dipole magnets, the effect of gas pressure on the separator transmission, and on the equilibrium charge of ions – products of the reactions ^{174}Yb, ^{206}Pb+^{48}Ca.

In November 2020, we started an experiment to study in detail the properties of Mc isotopes and their production cross sections in the complete-fusion reaction ^{243}Am+^{48}Ca.

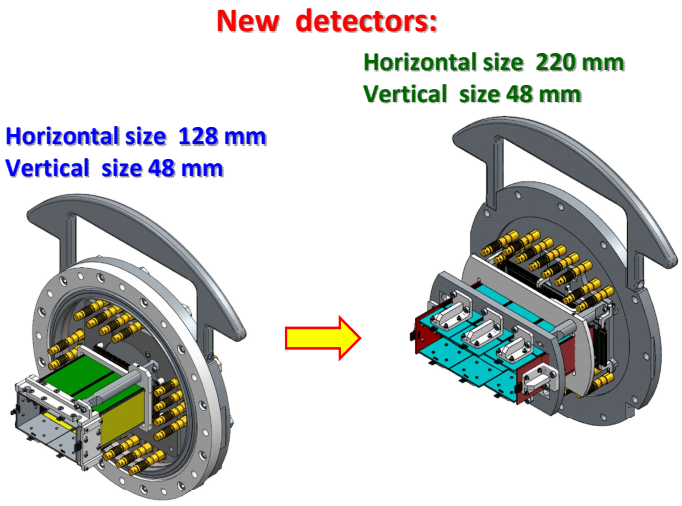

Fig. 12. Schematic image of the initially used and new detector arrays of the separator DGFRS-2.

Construction and commissioning of the pre-separator for radiochemical studies of SHE.

A new gas-filed separator, DGFS-3, (Fig. 13) is being developed for a detailed spectroscopic study of heavy isotopes. This separator is manufactured, equipped, and installed for testing at the beam of the DC280 cyclotron. High-beam intensities from the DC280 cyclotron and the increased detection efficiency of the modernized GABRIELA setup for gamma and conversion electrons will allow us to plan spectroscopy experiments in 2022 aimed at study the nuclear structure of superheavy nuclei. In the complete fusion reaction ^{48}Ca+^{243}Am→ ^{291}Mc*, we can reach a relatively high yield of one decay chain per day with the beam intensity of 1.5-2 pμA. During the experiment, we plan to measure about 100 decay chains of isotopes of element 115 consisting of 5 subsequent alpha decays

from Z=115 to 105. Coincidences with prompt and delayed gammas and conversion electrons will allow us to obtain information on the level structure of the populated isotopes.

Fig. 13. Separator DGFS-3 (during assembly) at the experimental hall of the SHE Factory.

It is planned to use the DGFS-3 setup for study chemical properties of SHE. For this purpose, the DGFS-3 is supplemented with an additional dipole magnet, before the focal plane, which will allow directing the beam of evaporation residues to a separate part of the setup for the radiochemical analysis.

Additionally, design work on a new setup, aimed solely at the study of the chemical properties of SHE has been started. We consider a gas-filled superconducting magnet for this purpose. Coupled with a reaction product collection chamber or a gas catcher, this set-up will serve as a pre-separator for further chemical separation.

Construction of the gas catcher

Since 2017, work has begun on the creation of a cryogenic gas ion trap designed to separate isotopes of heavy and superheavy elements synthesized in complete fusion reactions. The installation is supposed to be used at a factory of superheavy elements. A cryogenic gas ion trap is being created at FLNR in collaboration with the Max Planck Institute in Heidelberg (Germany). The construction was taken as a basis, implemented in Darmstadt for the SHIPTRAP installation [8]. A general view of the trap with its overall dimensions in the section is shown in Fig. 14. The actual gas cell 3, cooled to 40K, is placed in a vacuum volume 2. The gas cell contains a cylindrical eight-electrode transport system 4 and a radio-frequency multi-electrode cone 5. At the exit of the cell, a Laval nozzle 7 is installed, which forms a supersonic jet from a mixture of gas and ions and directs it into the volume where the pumping system evacuates the neutral gas, and the beam ions by the radio-frequency quadrupole transport system 8 is transferred to the next volume, where the next quadrupole system forms bunches from a continuous ion beam.

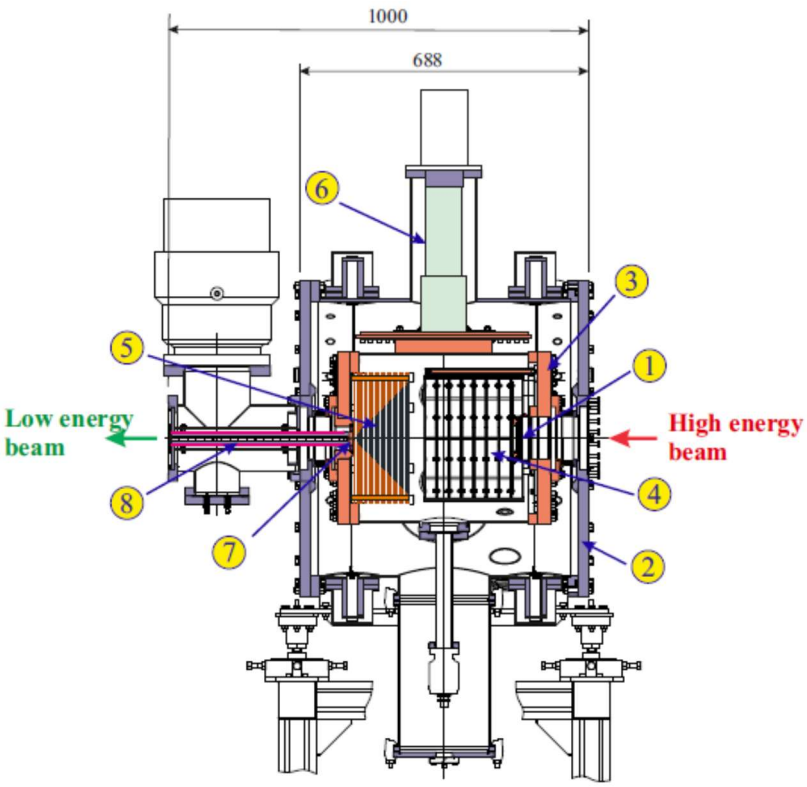

Fig. 14. General view of a cryogenic gas ion trap. Positions in the figure: 1 - entrance window; 2 - outer warm vacuum shell; 3 - cold inner chamber; 4 - cylindrical electrodes of a constant electric field; 5 - radio frequency multi-electrode cone; 6 - the head part of the cryo-refrigerator; 7 - supersonic nozzle; 8 - transport radio frequency quadrupole.

Figure 15 shows the vacuum diagram of the setup. The gas flow from the cell will be from 1 to 5 Torr·l/s, therefore the main pumping device is a turbomolecular oil-free pump with a capacity of 1600 l/s. A feature of such a pump is the ability to work with gas flows up to 16 Torr·l/s.

Table 6 shows the technical characteristics of the main equipment of the setup.

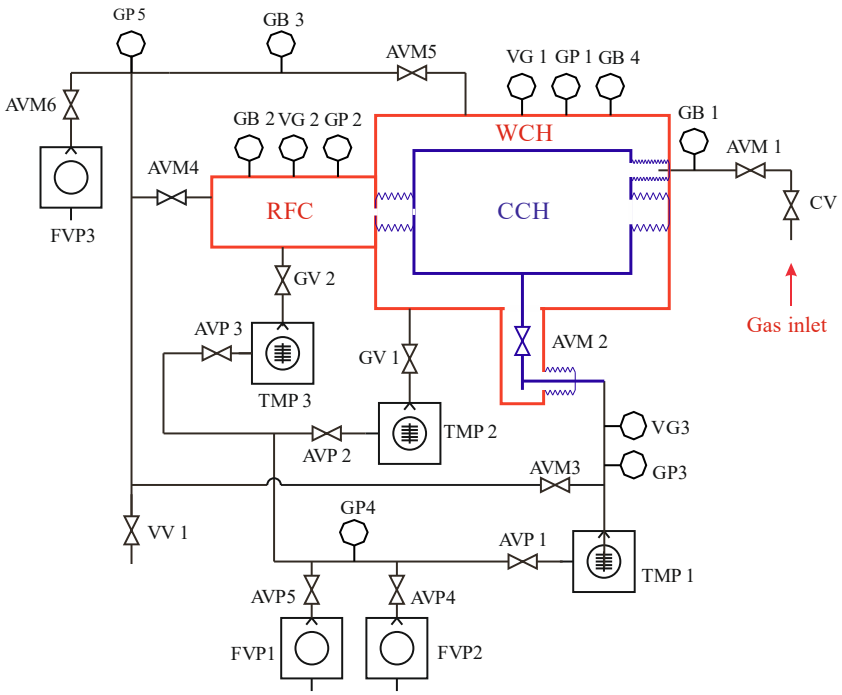

Fig.15. Vacuum scheme of the a cryogenic gas ion trap. CCH – cold chamber; WCH – warm chamber; RFC – radio-frequency chamber; GB1-GB4 – Baratron manometers; GP1-GP5 – Pirani vacuum gauge; VG1-VG3 – cold cathode vacuum gauge; TMP1-TMP3 – turbo molecular pumps; FVP-FVP3 – fore vacuum pumps; CV – control valve (MKS); AVM1-AVM3 – angle valves (manual); AVP1-ANP5 angle valves (pneumatic); VV1-VV3 – venting valves; GV1-GV3 – gate valves.

Table 6. Technical characteristics of the main equipment of the “Cryogenic gas ion trap” setup.

№	Element	Approximate dimensions, mm LxHxW	Mass, kg	Power consumption from the mains (kW);	Water cooling parameters (flow rate, t_{in}, P_{in})	Thermal power dissipated into the room (kW);	Noise level generated by operating equipment
1.	Double vacuum chamber	710x795x795	300 kg	-	-	-	
2.	Vacuum turbomolecular pumps HiPace® 300 M – 1 pc.	300x170x300	17,5	0,3	1,5 l/min 20–25^{0}C 5–6 Atm.	0,1	45 db
3.	Vacuum turbomolecular pumps HiPace® 700 M – 1 pc	300x210x300	21,0	0,3	2,0 l/min 20–25^{0}C 5–6 Atm.	0,1	45 db

4.	Vacuum turbomolecular pumps ATH1600MT – 1 pc.	400x400x500	40 kg	0,3	5 l/min 20–25^{0}C 5–6 Atm.	**0,12**	
5.	Forevacuum pumps XDS46i – 4 pc	750x500x420	55 kg each	0,52 each	Air Cool.	**2,08**	56 db each
6.	Cryorefrigerator	532x43x493	100	8 (3x380 V network)	10 l/min 20–25^{0}C 5–6 Atm.	**0,8**	
7.	2 equipment racks	500x700x2000 each	500 kg each	10 general	Air Cool.	**10**	~50 db general
8.	2 computers	200x500x400 each, plus monitors 500x500x200 each	10 kg each	3 kW general	Air Cool.	**1,5**	15 db each
9.	Gas cylinder (helium).	300x1500x300	50	-	-	**-**	-
						14,7	

*) – High vacuum and forevacuum pumps are powered from one of 2 equipment racks (see line 7 of this table). The power consumed by high-vacuum pumps is 0.9 kW, and by forevacuum pumps - 2.1 kW.

The maximum heat dissipation into the air is 14.7 kW.

During the reporting period, the following works were performed:

- Calculations of gas dynamics, radio frequency, and electrostatic transport systems.
- Preparation of the drawings of the vacuum volumes and the internal structure of the multi-electrode cell.
- The main elements of the structure have been manufactured.
- The necessary vacuum pumping equipment, measurements, fittings and accessories were purchased.
- The elements of the control and measurement system were purchased and tested.
- In 2020, the assembly of the main structure began, the warm chamber was pumped out to a pressure of 10^{-6} mbar.
- Currently, the acquisition and assembly of the multi-electrode system of the gas cell are underway.

Figures 16 and 17 show a photograph of the current state of the installation assembly.

Fig. 16. Assembling of the cryogenic gas ion trap.

Fig.17. The cryogenic gas ion trap

GALS – setup for on-line separation of transfer reaction products by selective laser ionization

Implementation of the GALS project, devoted to the production and study of heavy neutron-rich nuclei by multinucleon transfer reactions, is in progress. A series of computer simulations of radiofrequency ion guide, ion extraction system, Einzel lens, separator magnet (fig. 18) and electrostatic deflector (fig. 19) were performed [1-4] before their final design and production. A significant part of the subsystems is manufactured (e.g. front-end vacuum chamber, gas cell, radiofrequency ion guide, Einzel lens, mass-separator analyzing magnet, focal chamber, gas purifying system), although some of the parts are still being designed or manufactured (e.g. beam diagnostics, detection and DAQ systems).

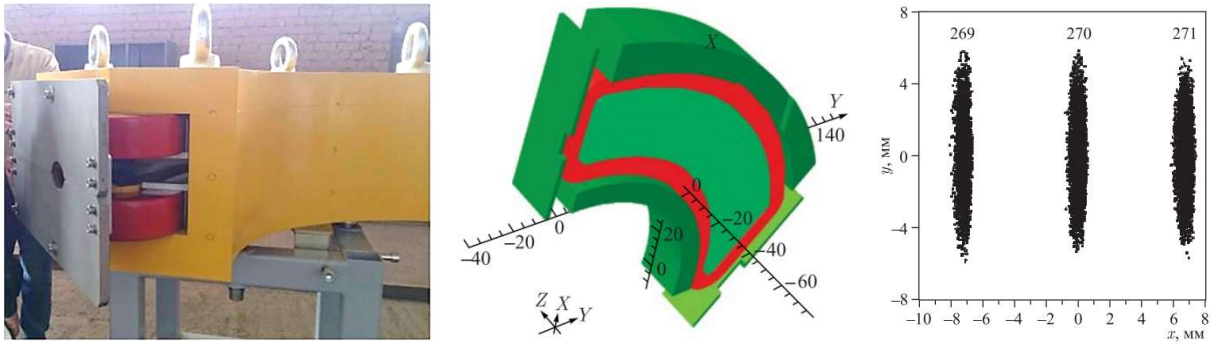

Fig. 18. The separator magnet, its computational model and distribution of ions of various masses in the focal plane of the spectrometer. Bending angle is 90°, equilibrium orbit radius ≈ 1 m, magnetic field 5000 gauss. The estimated mass resolution of the mass-separator R_m = 1400.

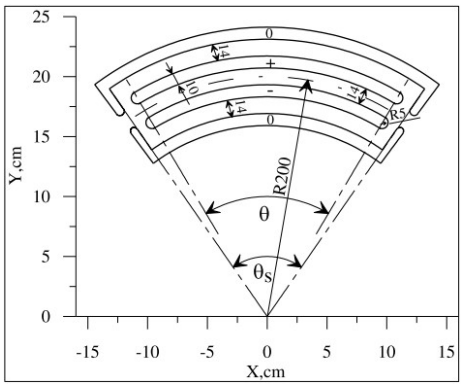

Fig. 19. Scheme of GALS electrostatic deflector. Bending angle is 67°, electrode voltages are U_1 = – 2.866 kV and U_2 = 2.754 kV, gap between the electrodes d = 14 mm, angular size of the potential electrodes θ = 62.6°, effective bending radius is 20.8 cm.

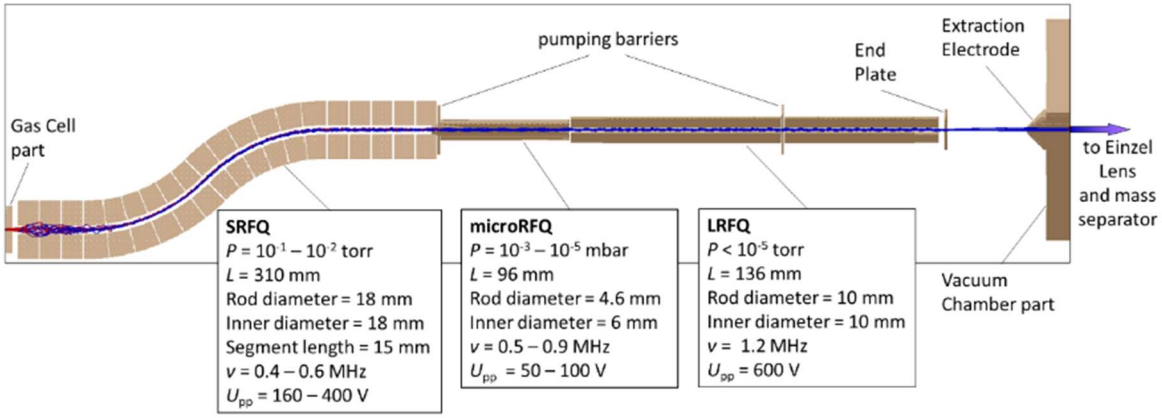

Fig. 20. The quadrupole ion guide SIMION model within the front-end vacuum chamber.

Radiofrequency quadrupole ion guide consisting of S-shaped segmented quadrupole, micro-RFQ and linear RFQ (see Fig. 20) was chosen to be used in the setup to transport the ions from the gas cell to the extraction electrode through differential pumping system. Compared to linear sextupole ion guide it showed significantly better transport time and efficiency during our SIMION simulations [5, 6]. The simulations predict ion transport time of 487.2 μs and efficiency up to 97 %. The system design and manufacturing were already completed (see Fig. 21) and it is currently at the stage of assembly and testing.

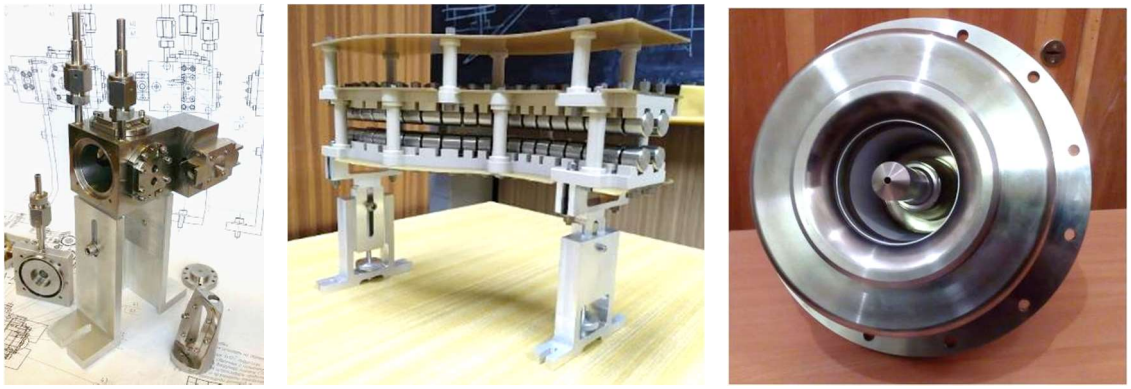

Fig. 21. The view of the gas cell (left), S-shaped part of the RFQ ion guide (center) and the ion extraction system (right).

First design of tape station for the detecting system was developed by our colleagues from South Africa and its prototype was manufactured in iThemba LABS. First test experiments and actual on-line work on gamma-spectroscopy of Yb isotopes were performed in order to determine deformation in these nuclei.

GALS laser laboratory preparation is almost finished. Most part of the laser equipment (TiSa and Dye lasers, beam diagnostics, doubling optics etc.) was delivered and now is being installed and tested.

Our laser system (see Table 7) is designed for 2- and 3-step non-resonant and resonant ionization of the atoms of interest. Lasers specified for non-resonant transition scheme are two tunable Credo Dye

lasers (Sirah Lasertechnik GmbH) pumped by two Nd:YAG INNOSLAB lasers (Edgewave GmbH). Credo laser has maximal average power of 27 W at fundamental wavelength and 3.8 W at second harmonic; its line width is 1.8 GHz at pulse duration about 7 ns. The laser wavelength can be stabilized to an external laser wavelength meter. The Edgewave Nd:YAG laser generates maximal average power of 92 W and 44 W for the second and third harmonic respectively (532 and 355 nm) with repetition rate 10 – 15 kHz and pulse duration of 8 – 10 ns. The divergence parameter of the green beam is $m^2 = 1.4$. Dye laser systems pumped by second and third harmonics of Nd:YAG provide tuning in a broad spectral range: from near UV to near IR.

Table 7. Laser to be used in multistep ionization. The lasers already installed and tested are presented in bold.

Type	Output power, main, (2^{nd}), {3^{rd}, 4^{th}} harmonic, W	Pulse frequency, Hz	Pulse length, ns	Wave length, nm
Edgewave Nd:YAG	**(92), {44}**	**10^4**	**8 – 10**	**532, 355**
Sirah Credo Dye laser	27, (3.8)	10^4	7 – 10	215 – 900
Photonics Industries Ti:Sapphire	**3, (1), {0.18, 0.07}**	**10^4**	**10 – 20**	**206 – 978**
Spectra-Physics Millennia Nd:YAG	**(10)**	**cw**	**cw**	**532**
Sirah Matisse Ring dye laser	**2.3, (0.6)**	**cw**	**cw**	**225 – 760**
M Squared SolsTiS Ti:Sapphire laser	5	cw	cw	725 – 960
Toptica TA Pro diode laser	0.5	cw	cw	649.9 – 657.1
Sirah Pulsed Dye Amplifier	0.9	10^4 (same as pump laser)	10 – 50 (same as pump laser)	374 – 900 (same as seed laser)

The generation of a Titanium-Sapphire lasers shifted to the red and infrared edge of the spectrum (680 – 960 nm) will be also used as complementary to that of the dye lasers. For this purpose three new TU-H pulsed tunable Ti:Sapphire lasers (Photonics Industries International, Inc.) were recently installed and tested. These lasers are equipped with second, third and fourth harmonic generation

units and provide a broad tuning range of 206-978 nm with average fundamental power up to 3 W. Optimization of their working parameters for performing our first off-line experiments is in progress.

A narrow-bandwidth laser system is intended for resonant transitions, e.g., for precise laser spectroscopy. It consists of a constant wave tunable Matisse ring dye laser (Sirah Lasertechnik GmbH) pumped by 10 W Millennia Nd:YAG laser (Spectra-Physics, Newport Corporation) and coupled with Sirah WaveTrain external cavity frequency doubler which allows a tuning range of 225 – 760 nm with power up to 2.3 W and linewidth of 200 kHz.

Our first offline experiments are planned to be performed on Os laser ionization with preliminary experiments on the best ionization scheme determination. For these offline experiments, our existing reference cell will be used and also a new more compact one will be built. Also, modernization of the vacuum pumping system of the existing reference cell is currently being performed.

References

[1] S. Zemlyanoy, K. Avvakumov, V. Fedosseev, R. Bark, Z. Blazczak, Z. Janas, Current status of GALS setup in JINR, Hyperfine Interactions, ISSN:0304-3843, eISSN:1572-9540, 238:31, 2017

[2] Sergey Zemlyanoy, Konstantin Avvakumov, Eduard Kozulin, Valentin Fedosseev, Robert Bark, Zenon Janas, Production and investigation of heavy neutron rich nuclei, EPJ Web of Conferences 163, 00065 (2017) (DOI: 10.1051/epjconf/201716300065)

[3] S Zemlyanoy, K Avvakumov, N Kazarinov, V Fedosseev, R Bark, Z Blazczak and Z Janas, Heavy neutron rich nuclei: production and investigation, IOP Conf. Series: Journal of Physics: Conf. Series 1023 (2018) 012004 (doi :10.1088/1742-6596/1023/1/012004)

[4] Kazarinov N., Kalagin I., Zemlyanoy S., Design and calculation of cylindrical electrostatic deflector for the transport channel of the heavy ion beam, Proceedings of RuPAC2016, St. Petersburg, Russia, ISBN 978-3-95450-181-6

[5] Sergey Zemlyanoy, Konstantin Avvakumov, Batsuren Zuzaan, Yury Kudryavtsev, Valentine Fedosseev, Robert Bark, Zenon Janas, Further development of GALS setup at JINR, Hyperfine Interactions 241 (2020) 38 (https://doi.org/10.1007/s10751-020-1707-3)

[6] S Zemlyanoy, K Avvakumov, G Myshinsky, V Zhemenik, Yu Kudryavtsev, V Fedosseev, R Bark and Z Janas, Production and study of neutron rich heavy nuclei, GALS setup, Journal of Physics: Conference Series 1555 (2020) 012021 (doi:10.1088/1742-6596/1555/1/012021)

Development of the ACCULINNA-2 separator

ACCULINNA-2 is a part of the Dubna Radioactive Ion Beams (DRIBs) project [1–3]. The separator was commissioned in 2017 as a result of successful collaboration with the SIGMAPHI company [5]. This new in-flight facility was installed at a primary beam line of the U-400M cyclotron

for the study of exotic nuclear systems with atomic number Z < 20 [2,4] (Fig. 22). The separator provides high-quality secondary beams and opens new opportunities for the experiments made with the RIBs of the intermediate energy range (E ~ 5÷50 MeV/nucleon) [3]. Measured characteristics of the radioactive ion beam (RIB) (intensity, purity, beam profiles in all focal planes) are in good agreement with the project assumptions [1-4].

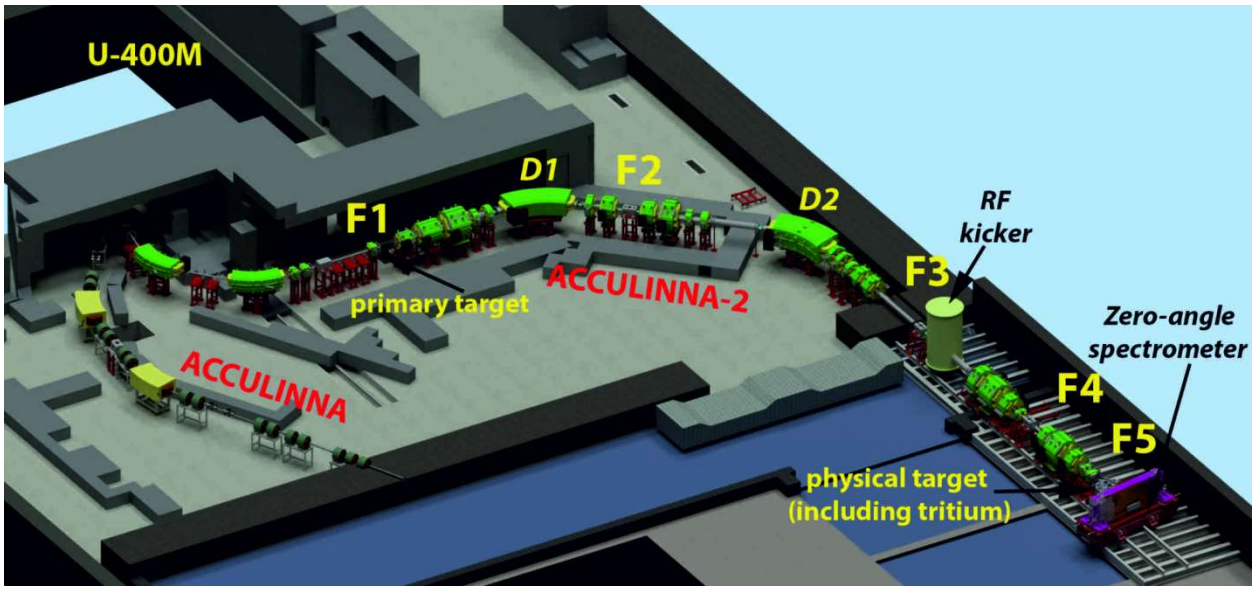

Fig.22. Layout of the ACCULINNA-2 fragment-separator at U-400M cyclotron hall.

In 2017-2021 several methodical works aimed to preparation to the full scale experiments with ^{6}He, ^{8}He, ^{9}Li, ^{10}Be, ^{27}S, and other beams were carried out [5-12]. In 2017 the dipole magnet of the zero degree spectrometer had been installed at the ACCULINNA-2 beamline (Fig. 23). A significant financial contribution to the zero degree spectrometer project was from polish plenipotentiary representative grants at JINR. Further, a particle tracking system based on parallel plate avalanche counters (PPAC) and a double-sided silicon strip detector for the spectrometer are being developed.

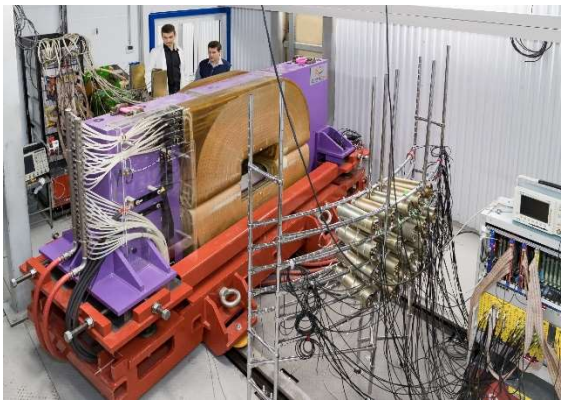

Fig.23. Dipole magnet of zero degrees spectrometer at the ACCULINNA-2.

In 2018-2020, the development of essential experimental equipment for the ACCULINNA-2 beam line was continued. One of the most significant developments was the design and installation

of the radio-frequency filter (RF kicker). The RF kicker, with maximal electric field amplitude of 15 kV/cm and frequency in the range of 14.5-20 MHz, should provide a significant improvement of RIBs purity (by a factor of 5÷20 in depending on the ion) [1]. Technical parameters and a side view of the RF kicker are presented in Fig. 24. Experiments with the purified RIBs (e.g., ^{15}O, ^{17}Ne, ^{28}S, etc.) will be performed after the U400M cyclotron upgrades since the end of 2022.

Frequency range (MHz)	14.5 – 20
Peak voltage (KV)	120
Gap (mm)	170
Width of electrode (mm)	120 min
Length of electrodes (mm)	700
Cylinder diameter (mm)	1200 max
Stem diameter (mm)	120 max
Length of coaxial line (mm)	1830
Distance from A-2 primary target (m)	25

Fig. 24. The principal parameters and a side view of the RF kicker installed at the ACCULINNA-2 beam line after the achromatic focal plane F3.

An initial step of preparation for the experimental studies of light neutron-rich systems, in 2019, the project of the tritium target complex has been started. The project is developed in a collaboration with VNIIEF (Sarov), DZHM (Dzerzhinsk), and VNIPIET (Sosnoviy Bor). A conceptual design of the tritium-target complex (Fig. 25) is established.

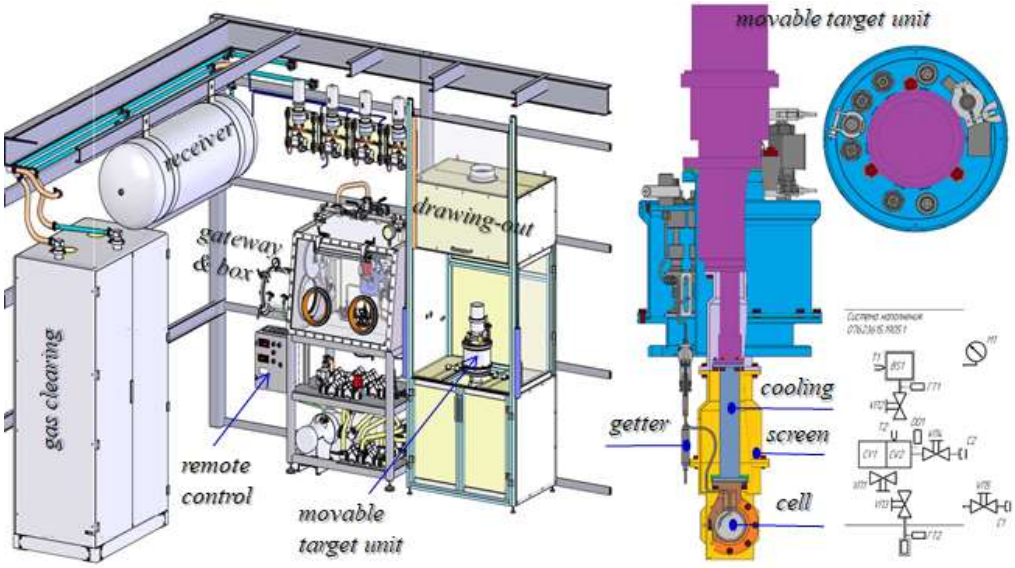

Fig. 25. Scheme of the gas-vacuum system (left) and the tritium target cell with related subsystems (right).

It includes a comprehensive gas-vacuum and tritium safety system for the supply, cooling-heating, control, radiation safety, and utilization of unwanted gases. The design of the cryogenic tritium target cell, gas vacuum system is on the stage of the equipment ordering and manufacturing.

The technical design of the experimental cabin is under technical expertise for safety rules before approval. The complex will provide operation at gaseous and liquid targets at cryogenic temperatures. As a result, the targets of all long-living isotopes of hydrogen (including tritium) and helium with the thickness being in a wide range ($10^{20} \div 5*10^{21}$ atoms/cm^2) will be available for use in experiments since the end of 2023.

New detector systems and related electronics have been developed as well. They include the following items: a) detector array for detection of neutrons based on stilbene crystals [5] and scintillation fibers [6]; b) radiation-hard and extremely fast silicon strip detectors providing excellent time resolution ($\sigma \sim 50$ ps) for RIB diagnostics [7-9]; c) scintillation arrays of CsI(Tl), $LaBr_3$(Ce), etc. crystals for detection of gamma-rays and possible detection of charged particles; d) new generation of micro-strip silicon detectors dedicated intended for tracking of charged particles [6]. Actually, the zero-angle spectrometer, together with hodoscope detectors and neutron array at the final focal plane F5, is under construction.

The neutron spectrometer based on 64 stilbene crystals is intended to identify neutrons in the energy range from a few to tens of megaelectronvolts. The stilbene crystals of 80 mm in diameter with 50 mm thickness were produced at Amcrys-H (Kharkiv, Ukraine). As a result, the neutron spectrometer was successfully used in the ^{9}Li(d,p)^{10}Li $\rightarrow$ n+^{9}Li reaction [11] for coincidence measurements of ^{9}Li, and neutrons emitted at forward angles. For precise measurement of neutron energy and emission angle, the array of 48 detection modules [5] was used (Fig. 26). Among the advantages of such modules belongs: excellent n-γ separation available at the energy > 200 keV (electron scale) and very good timing resolution (better than 0.5 ns since the energy 300 keVee), see Fig. 27. At the same time, the neutron detection efficiency is sufficiently high: namely, it equals 18% and 30% for neutrons with energies of 10 MeV and 4 MeV, respectively.

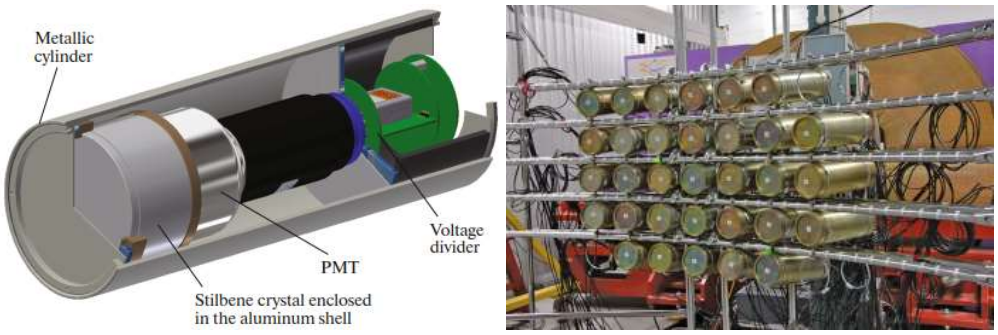

Fig. 26. A scheme of detecting module in the neutron spectrometer and the neutron spectrometer assembly.

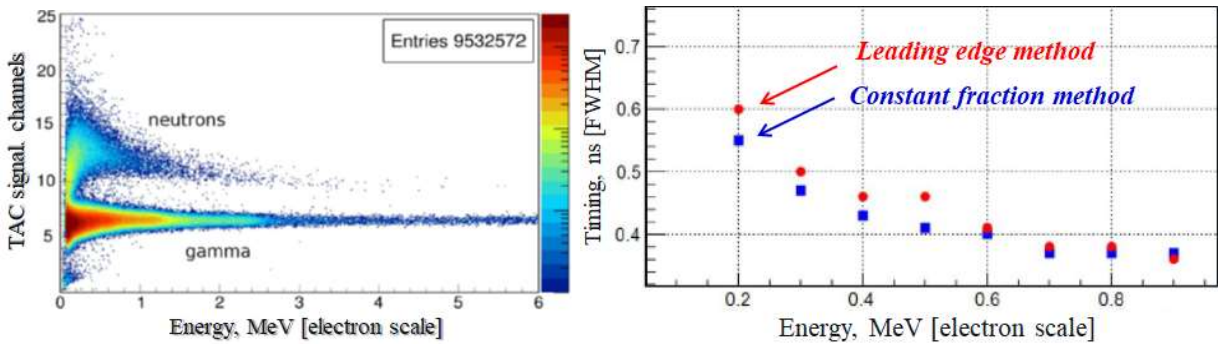

Fig. 27. The typical quality of n-γ separation for stilbene based detectors (left panel) and timing resolution as a function of energy (right panel). Data was obtained with the use ^{252}Cf source.

One of the essential aspects for detection of ^{9}Li populated in ^{10}Li decay was the developed time of flight (ToF) detector consisting of the thin scintillator EJ-212 (125 μm) and four Hamamatsu R7600 photomultiplier tubes. This detector, placed at a distance of 39 cm downstream the physical target, allowed one to identify the components of the secondary beam (mainly d, ^{6}He, ^{9}Li and ^{12}Be) by ΔE-ToF method and separate the ^{9}Li isotopes from the beam from those populated in the ^{10}Li decay.

The new project of the Active Gaseous Target – Time Projection Chamber (AGT-TPC) is started in collaboration with the Faculty of Physics, UW, Warsaw, to build universal instrumentation for the study of structure and decays of the most exotic nuclei. The AGT-TPC is a novel gas-filled detection system in which a gas volume acts as a tracking medium and a target simultaneously. The vacuum vessel of the AGT-TPC is already manufactured, and the low-pressure gas system is already designed, mounted, and tested (Fig. 28). The low-pressure gas system is already implemented to the ACCULINNA-2 control for PPAC detectors for particle trackings in the area of the F5 focal plane.

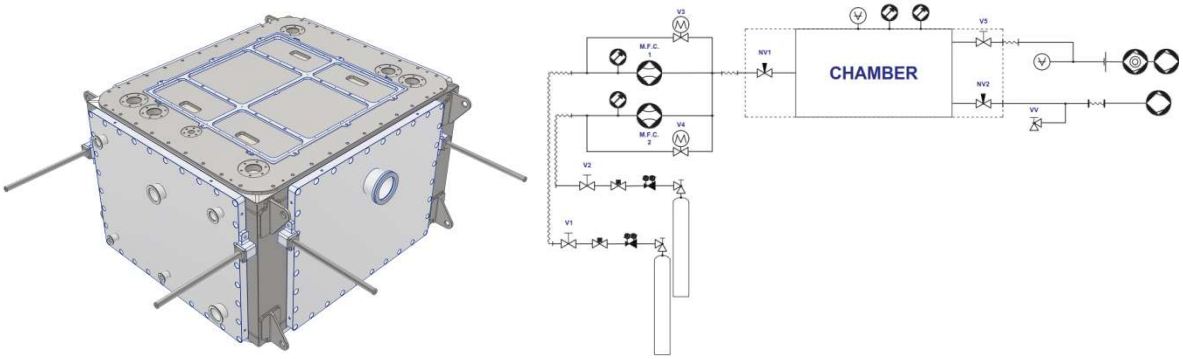

Fig. 28. A schematic view of the vacuum vessel (left) and the low-pressure gas system (right) of the AGT-TPC.

The automation and safety systems consisting of a number of control and monitoring elements and related software have been developed for the following subsystems: vacuum, magnet power supply, beam monitoring, high voltage power supply for the detectors.

Important software packages have been developed in collaboration with the Laboratory of Information Technologies. I. ExpertRoot (er.jinr.ru) – the FairRoot based simulation, reconstruction, and data analysis package. A number of original, sophisticated algorithms are implemented for the detector geometry description, ion propagation through geometry, interaction sampling, particle identification, and reconstruction. II. The AccDaq library allows flexible and fail-safe configuration of the MBS-based (gsi.de/mbs) readout setup, data repacking, and conversion to Root. The same configuration file is used for configuring electronics, converting data, and building the output data Root class compatible with Go4 (gsi.de/go4) and ExpertRoot packages.

References

[1] A.S. Fomichev, L.G. Grigorenko, S.A. Krupko, S.V. Stepantsov, G.M. Ter-Akopian, *"The ACCULINNA-2 project: The physics case and technical challenges",* Eur. Phys. J. A **54** (2018) 97.

[2] A.A. Bezbakh, W. Beekman, V. Chudoba, A.S. Fomichev, M.S. Golovkov, A.V. Gorshkov, L.V. Grigorenko, G. Kaminski, S.A. Krupko, M. Mentel, E.Yu. Nikolskii, Yu.L. Parfenova, P. Plucinski, S.I. Sidorchuk, R.S. Slepnev, P.G. Sharov, G.M. TerAkopian, B. Zalewski, *"First radioactive beams at ACCULINNA-2 facility and first proposed experiment",* EPJ Web of Conferences 177 (2018) 03001.

[3] A. S. Fomichev, A. A. Bezbakh, S. G. Belogurov, R. Wolski, E. M. Gazeeva, A. V. Gorshkov, L. V. Grigorenko, B. Zalewski, G. Kaminski, S. A. Krupko, I. A. Muzalevskii, E. Yu. Nikolskii, Yu. L. Parfenova, S. I. Sidorchuk, R. S. Slepnev, G. M. Ter-Akopian, V. Chudoba, and P. G. Sharov, *"The first experiments with the new ACCULINNA-2 fragment separator",* Bulletin of the Russian Academy of Sciences: Physics, **83** (2019) 385–391.

[4] G. Kaminski, B. Zalewski, S.G. Belogurov, A.A. Bezbakh, D. Biare, V. Chudoba, A.S. Fomichev, E.M. Gazeeva, M.S. Golovkov, A.V. Gorshkov, L.V. Grigorenko, D.A. Kostyleva, S.A. Krupko, I.A. Muzalevsky, E.Yu. Nikolskii, Yu.L. Parfenova, P. Plucinski, A.M. Quynh, A. Serikov, S.I. Sidorchuk, R.S. Slepnev, P.G. Sharov, P. Szymkiewicz, A. Swiercz, S.V. Stepantsov, G.M. Ter-Akopian, R. Wolski,*"Status of the new fragment separator ACCULINNA-2 and first experiments",* Nucl. Instrum. Methods Phys. Res. B **463** (2020) 504-507.

[5] А. А. Безбах, С. Г. Белогуров, Р. Вольски, Э. М. Газеева, М. С. Головков, А. В. Горшков, G. Kaminski, М. Ю. Козлов, С. А. Крупко, И. А. Музалевский, Е.Ю. Никольский, Е. В. Овчаренко. Р. С. Слепнев, Г. М. Тер-Акопьян, А. С. Фомичев, В. Худоба, П.Г. Шаров, В. Н. Щетинин, *"Нейтронный спектрометр для проведения экспериментов с радиоактивными пучками на фрагмент-сепараторе АКУЛИНА-2",* ПТЭ **5** (2018) 1-8; Bezbakh A.A. et al., *"A*

neutron spectrometer for experiments with radioactive beams on the ACCULINNA-2 fragment separator", Instrum. Exp. Tech., Vol. **61** (2018) 631-638.

[6] V. Chudoba for the EXPERT project, *"The EXPERT project: part of the Super-FRS Experiment Collaboration",* J. Phys.: Conf. Ser. **1024** (2018) 012021; http://aculina.jinr.ru/expert.html

[7] V. Eremin, A. Bezbakh, I. Eremin, N. Egorov, A. Fomichev, M. Golovkov, A. Gorshkov, A. Galkin, O. Kiselev, A. Knyazev, D. Kostyleva, S. Krupko, D. Mitina, Slepnev, P. Sharov and E. Verbitskay, *"Beam tests of full-size prototypes of silicon detectors for TOF heavy-ions diagnostics in Super-FRS"*, Journal of Instrumentation, **12** (2017) C03001.

[8] V. Eremin, D. Mitina, A. Fomichev, O. Kiselev, N. Egorov, I. Eremin, A. Shepelev, E. Verbitskaya, *"A comparative study of silicon detector degradation under irradiation by heavy ions and relativistic protons",* Journal of Instrumentation, **13** (2018) 01019.

[9] D. Kostyleva, O. Kiselev, A. Bezbakh, V. Chudoba, V. Eremin, A. Fomichev, A. Gorshkov, S. Krupko, I. Mukha, I. Muzalevskii, C. Scheidenberger, P. Sharov,*"Study of the silicon detectors for time-of-flight measurements at the SuperFRS facility and EXPERT experiments at FAIR",* ACTA PHYSICA POLONICA B **49** (2018) 503.

[10] I.A. Muzalevskii, V. Chudoba, S.G. Belogurov, A.A. Bezbakh, D. Biare, A.S. Fomichev, S.A. Krupko, E.M. Gazeeva, M.S. Golovkov, A.V. Gorshkov, L.V. Grigorenko, G. Kaminski, O. Kiselev, D.A. Kostyleva, M.Yu. Kozlov, B. Mauyey, I. Mukha, E.Yu. Nikolskii, Yu.L. Parfenova, W. Piatek, A.M. Quynh, V.N. Schetinin, A. Serikov, S.I. Sidorchuk, P.G. Sharov, R.S. Slepnev, S.V. Stepantsov, A. Swiercz, P. Szymkiewicz, G.M. Ter-Akopian, R. Wolski, B. Zalewski, *"Detection of the low energy recoil ^{3}He in the reaction ^{2}H(^{8}He,^{3}He)^{7}H",* Bulletin of the Russian Academy of Sciences: Physics, **84** (2020) 500-504.

[11] A.A. Bezbakh, S.G. Belogurov, D. Biare, V. Chudoba, A.S. Fomichev, E.M. Gazeeva, M.S. Golovkov, A.V. Gorshkov, G.Kaminski, S.A. Krupko, B. Mauyey, I.A. Muzalevskii, E.Yu. Nikolskii, Yu.L. Parfenova, W. Piatek, A.M. Quynh, A. Serikov, S.I. Sidorchuk, P.G. Sharov, R.S. Slepnev, S.V. Stepantsov, A. Swiercz, P. Szymkiewicz, G.M. Ter-Akopian, R. Wolski, B. Zalewski, *"Study of ^{10}Li low energy spectrum in the ^{2}H(^{9}Li,p) reaction",* Bulletin of the Russian Academy of Sciences: Physics, **84** (2020) 491-494.

[12] G. M. Ter-Akopian, Yu. Ts. Oganessian, A.A.Bezbakh, A. S. Fomichev, M. S. Golovkov, A.V. Gorshkov, S.A. Krupko, E. Yu. Nikolskii, S. I. Sidorchuk, S.V. Stepantsov, R. Wolski, *"Radioactive-ion beams for the fission study of heavy neutron-rich nuclei",* Physics of Atomic Nuclei, 2020, Vol. **83**, No. 4, 497–502.

Spectrometer MAVR

In 2019, a high-resolution magnetic analyzer (MAVR) was created and launched on the beam of the U 400 cyclotron of the FLNR, JINR (see fig. 29).

The MAVR analyzer has a large energy range for registering the products of nuclear reactions, a relatively large solid angle, and a high resolution. The analyzer maintains linearity in the focal plane over the entire length of 1500 mm as well as linear dependence of dispersion and resolution on the position in the focal plane. The length of the particle trajectory in the separator makes it possible to analyze rather short-lived (~ 0.5 μs) products of nuclear reactions.

The main parameters of the spectrometer:

1. Average radius of the orbit: 1.25 m
2. Deflection angle: 110.70
3. Magnetic rigidity: 0.5 - 1.4 Tm
4. Energy range: 5.2
5. Resolution :2000
6. Dispersion: 1.9 cm /%
7. Solid angle: up to 5 msr

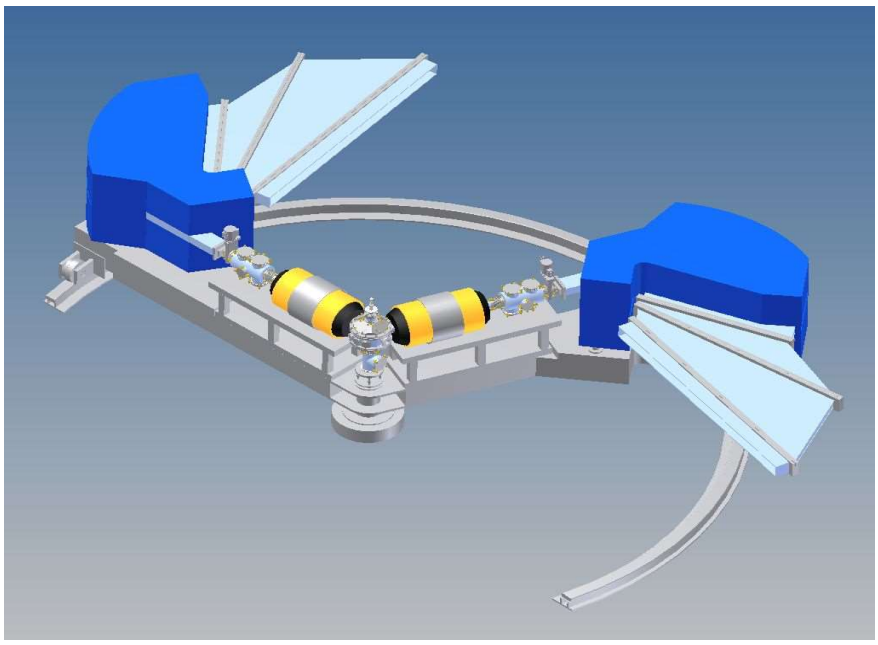

Fig. 29. Scheme of the high-resolution magnetic analyzer (MAVR).

Work continued on development of methods for registering the products of nuclear reactions with stable and radioactive nuclear beams. For the MAVR setup, a multi-detector spectrometer MULTI has been created which includes 10 detectors based on CeBr3 scintillators and 40 He3 neutron counters (see Fig. 30). This spectrometer will be used to measure decays of nuclei formed in

the reactions with emission of fast particles. For the MAVR magnetic analyzer, a time-of-flight system has been created for identifying reaction products and measuring their masses.

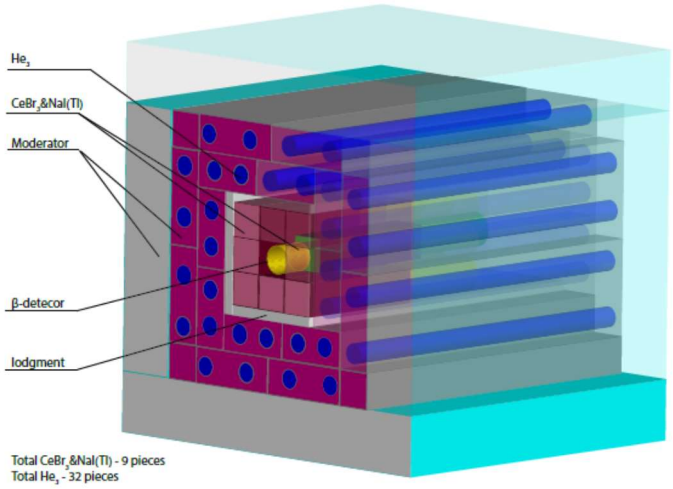

Fig. 30. Scheme of arrangement of detectors in the MULTI setup.

The composition of the detector group includes:

Detector	solid angle	resolution		eff.	number
		energy	angle		
Segmentation high resolution gamma ray detectors (CLOVER)	-	~3 keV	-	5%	2
$CeBr_3$ detectors of γ-quanta	4π	~20 keV	-	30%	10
Scintillation β-detector	~ 4π	-	-	60%	1
CeBr3 + NaI (Tl) β-detector	~ π	1 MeV	-	10%	1
^{3}He neutron detector	~ 4π	-	20°	25%	40

CONSTRUCTION OF A PROTOTYPE OF THE INITIAL SECTION OF A HIGH-CURRENT HEAVY-ION LINEAR ACCELERATOR AIMED AT PRODUCING INTENSE RADIOACTIVE ION BEAMS FOR BASIC RESEARCH

Development of systems with the radiofrequency quadrupole focusing (RFQ) functioning in the continuous mode (CW) is the general trend of the accelerator technique aimed on the production of high quality radioactive beams, see [1] and refs. therein. These systems are used for bunching and acceleration of a beam in the initial part of the accelerating complex up to energies of several MeV, provide possibility of low-energy (down to several tens of keV) injection of ion beam and allow for high (close to 100 %) beam transmission efficiency. Today in the world, the technology of creation of CW-RFQ is still under development. There are already examples of the operating CW-RFQ but so far working with beams of negligibly small intensity.

As a first step of R&D the design of RFQ with 4-vanes structure was carried out in 2020/21. Geometry and main dimensions of one chamber are shown in the Fig. 31. It assumes that all parts must be machined from Oxygen Free Electronic Copper and assembled into one construction via brazing. One section of resonator consists of four separate electrodes. Modulation must applied on the tip of every electrode. Vertexes of modulation must be machined with 25μ precision according to coordinates known from electrodynamic calculations. Electrodes must have cooling channels inside. It is allowed to make them via brazing from several parts. This resonator can be manufactured by European supplier in the end 2021.

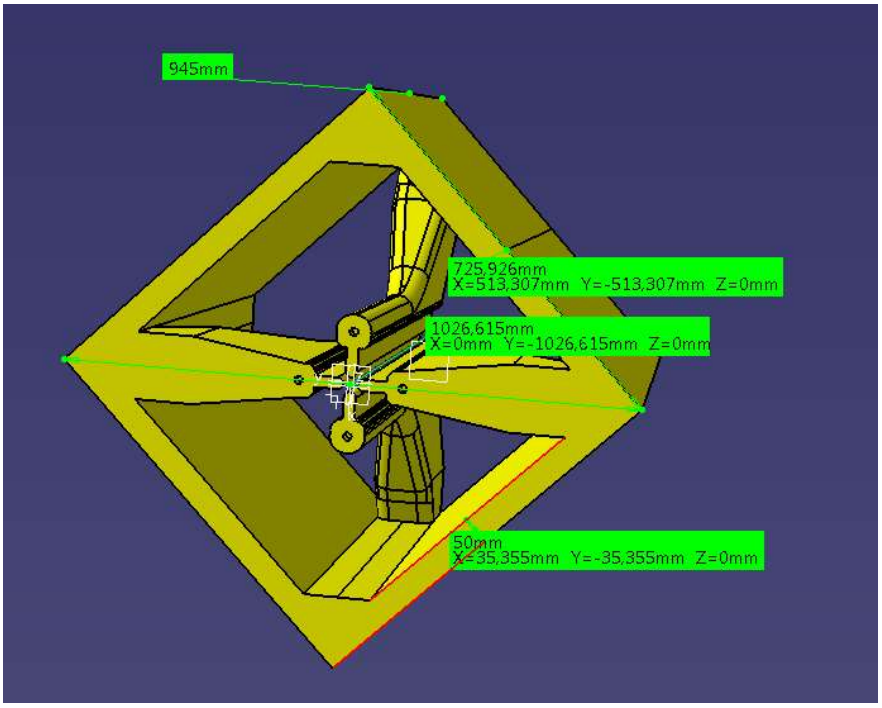

Fig. 31. “Diagonal” geometry for 4-vanes RFQ resonator.

The RFQ beam dynamics simulation was carried out for ion beams with A/Z ≤7.5 where A and Z are the ion atomic mass and charge state. The beam current for simulation was 1 mA. The result of beam dynamics simulation is presented in Fig. 32.

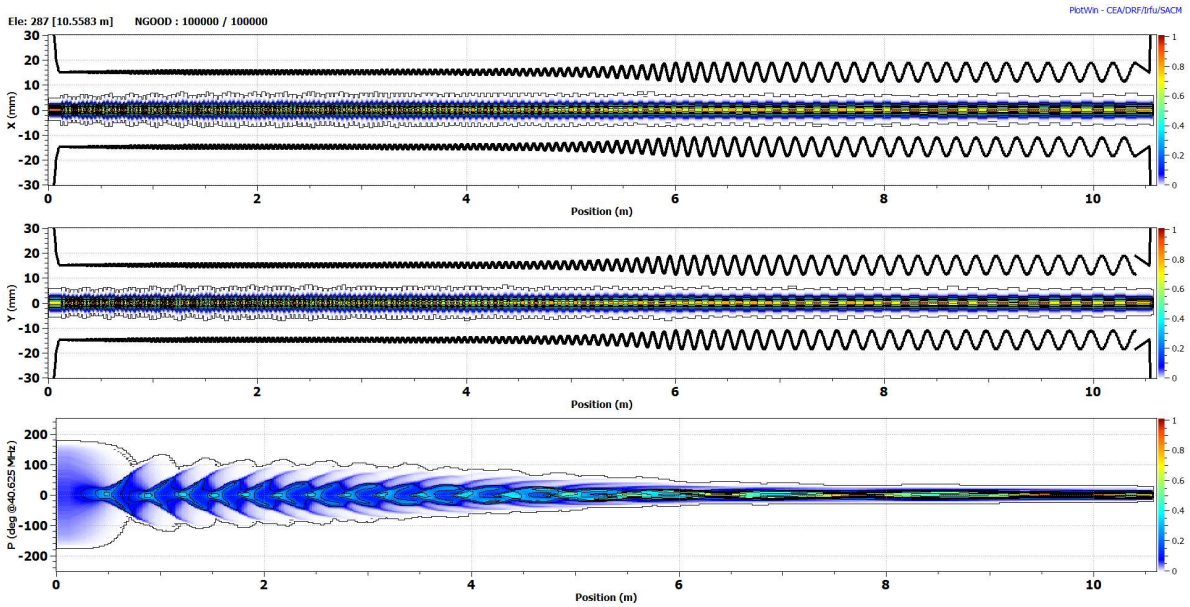

Fig. 32. Result of beam dynamics simulation for RFQ.

The resonator for RFQ with 8-vanes structure (Fig. 33) was developed using the results of beam simulation. For sizes listed in Tab. 8 the main RF parameters are:

- self-quality factor = 11300;
- RF power = 24.3 kW/cell = 25.7 kW/m;
- dipole mode ≈ 46 MHz.

Table 8. The main RFQ cell sizes.

Inner diameter, mm	720
Cell length, mm	945
Electrode`s base width, mm	120
Windows length, mm	750
Windows height, mm	210

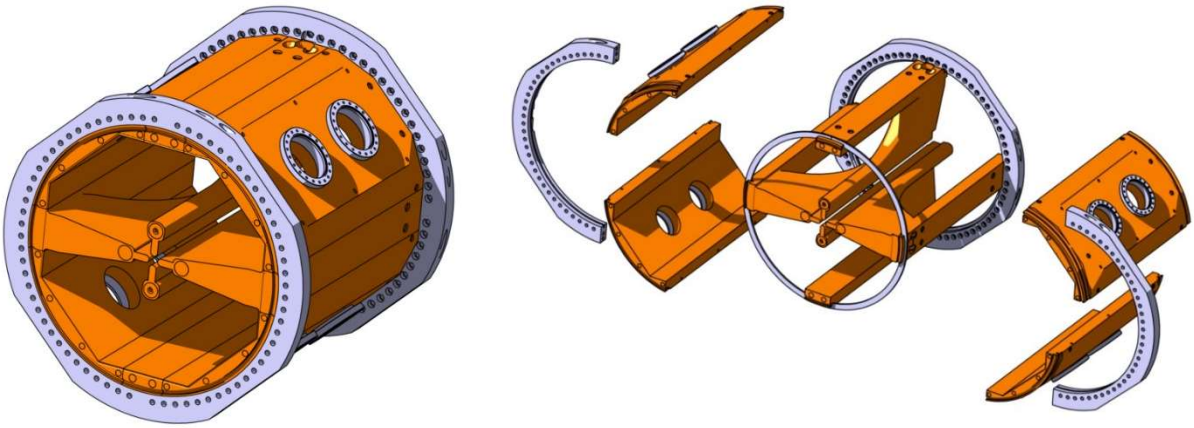

Fig. 33. Sketch of CW-RFQ section for operating with intensive heavy ion beams.

[1] L.V. Grigorenko, G.N. Kropachev, T.V. Kulevoy, I.N. Meshkov, S.M. Polozov, A.S. Fomichev, B.Yu. Sharkov, P.Yu. Shatunov, M.I. Yavor, DERICA project and strategies of the development of low-energy nuclear physics, Physics of Atomic Nuclei, Vol. 84 (2021) 50-63.